Chaos, Solitons and Fractals 84 (2016) 81–87

Contents lists available at ScienceDirect

Chaos, Solitons and Fractals

Nonlinear Science, and Nonequilibrium and Complex Phenomena

journal homepage: www.elsevier.com/locate/chaos

Differential equation of a fractal electrode–electrolyte interface

Carmelo José Felice*, Gabriel Alfredo Ruiz

Laboratorio de Medios e Interfases, Departamento de Bioingeniería, UNT/CONICET, CC 327-Correo Central, 4000 Tucumán, Argentina

ARTICLE INFO

Article history:
Received 7 August 2015
Accepted 7 January 2016
Available online 3 February 2016

Keywords:
Electrodes
Electrochemistry
Impedance
Fractal
Differential

ABSTRACT

Understanding an electrode–electrolyte interface (EEI) behavior is a valuable tool in several areas of science. There are models based on discrete fractal structures, which explain the measurements of linear and non-linear impedance at fixed frequencies, or at determined ranges of high and low current densities. A level by level discrete calculation is needed to evaluate these models, or the use of *black-box* models, which affect the good understanding of the phenomenon. A continuous model based on a differential equation of an EEI is presented in this paper. It includes an electrical circuit similar to a long transmission line. It has been deduced from the discrete Liu model.

1. Introduction

Understanding an electrode–electrolyte interface (EEI) behavior is a valuable tool in several areas of science. For instance, when measuring pH or bacterial concentration [1–3], or when recording electrocardiogram (*ECG*), electroencephalogram (*EEG*) or electromyogram (*EMG*) [3]. Besides, it is essential to understand how it interferes with measurements when the interface is operating in the non-linear zone, such as the non-linear dielectric spectroscopy of biological suspensions [2].

In all cases, it is necessary to deeply understand the electrode behavior, mainly when it is in contact with a biological tissue or cells in suspension.

Physically, the electric current encounters Ohmic resistances in both media (metal and electrolyte), and a capacitance through the interface.

On the other hand, polished surfaces usually show scraping lines under magnification. These grooves have been modeled as distributed RC elements [4,5].

The cross section of the interface model is shown in Fig. 1a, where the electrolyte is depicted in black. The grooves in the electrode can be seen as projections on the electrolyte side. Each groove has a self-similar structure, that is, it is divided into two branches ($N=2$) and these are similar to the original groove (hence the name of self-similar) when magnified by a factor $\boldsymbol{a}$, with $\boldsymbol{a} > N \geq 2$ [13].

The reader would recognize this model as the Cantor-bar fractal structure.

The equivalent electric circuit is shown in Fig. 1b represented in 3D. In it, the electrolytic resistance (R) is increased by a factor a in each subdivision, since at this ratio the cross section is reduced. Z_p represents the impedance of the EEI (of the two side faces of the branches) and it is modeled as the double layer capacity C_{dl} in parallel with the charge transfer resistance R_{ct}. Z_p is the same at each fractal level. The common ground of the circuit is the electrode.

This model includes two electrochemical parameters (C_{dl} and R_{ct}) incorporated in the geometric structure of the electrode. The charge transfer resistance R_{ct} has been incorporated to take into account redox processes.

Since the circuit components of Fig. 1 have the same value, it can be assumed that there are equipotential points

* Corresponding author. Tel./fax: +54 381 4364120.
E-mail address: cfelice@herrera.unt.edu.ar (C.J. Felice).

http://dx.doi.org/10.1016/j.chaos.2016.01.003
0960-0779/

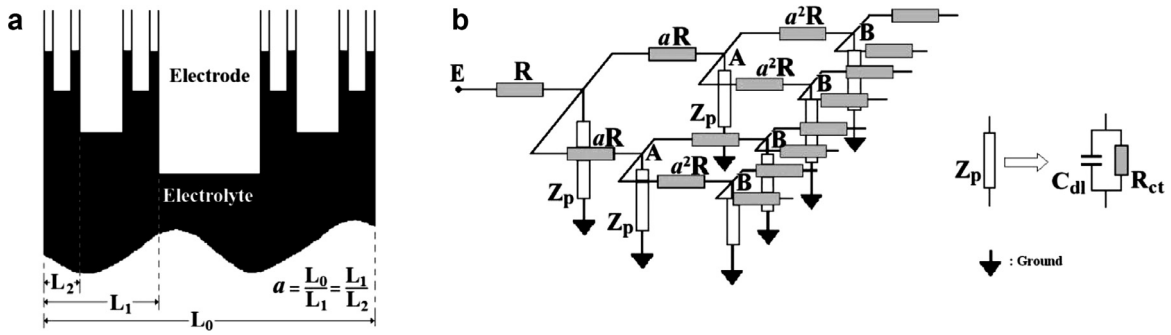

Fig. 1. (a) Cantor-bar fractal model of a rough-EEI, showing two grooves each with four fractal levels. The electrode is shown in white while the electrolyte in black. (b) Equivalent electric circuit for the fractal net of the rough-EEI in a three-dimensional way. *R*: electrolytic resistance, *a*: scale factor, R_{ct}: charge transfer resistance and the C_{dl} double layer capacity. A and B are equipotential points.

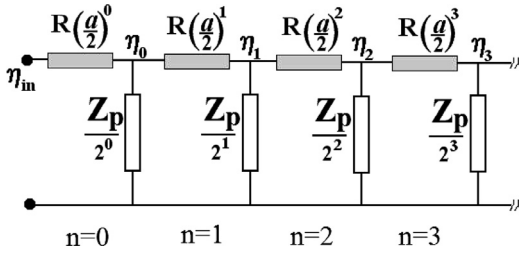

Fig. 2. Simplified fractal net showing the first four levels. *R*, Z_p and *a* idem Fig. 1, $\eta_{0,1,2,3}$ overpotential at different fractal levels ($n=0$ correspond to a flat electrode, $n=1$ to first fractal level, and so on).

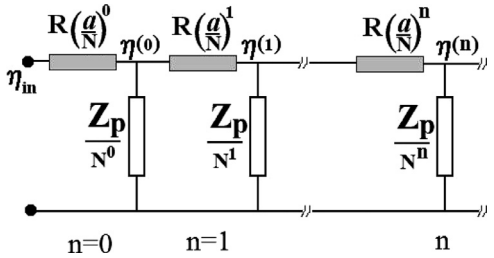

Fig. 3. Generalized discrete model of Fig. 2 considering *N* bifurcations by level and $\eta(n)=\eta_n$; $n=0,1,2\ldots$.

at every level [6], i.e., A corresponds to the first level, B to the second, and so on. Due to this equipotentiality, the circuit can be simplified as shown in Fig. 2.

It is possible to generalize the discrete model of Fig. 2, if N branches or bifurcations are considered by level for each level, instead of two (see Fig. 3).

Thus, a low value of N indicates a high roughness surface, because the grooves need more fractal levels to reach the molecular size. In the case where it is desired to calculate the voltage in every stage, the model has to be developed up to the desired stage. In the reviewed literature, the number of fractal levels of a surface has been modeled by a discrete variable [4,5,7–9].

In this paper we present a non homogeneous second order differential equation with constant coefficients to describe the behavior of an electrode–electrolyte interface. It has been obtained by replacing a discrete fractal model [4,5], by a quadrupole based model similar to a long transmission line. An analytic solution for a simplified version of the differential equation is presented.

The proposed continuous model predicts the potential's changes depending on the distance to the electrode arising from the roughness of the material, but does not report on what happens inside the double layer.

2. The model

It can start from the model of an EEI described by Ruiz et al. [4,5] and shown in Fig. 3. On it, the discrete variable n indicates the fractal level considered ($n=0$ correspond to a flat electrode, $n=1$ to first fractal level, and so on), *a* is the value that divides the channel width of a level to move on to the next one, and N is the number of branches or bifurcations considered by level.

The value of the parallel impedance for each fractal level ($n=0,1,2$, etc.) is:

$$Z_p = \frac{-jX\ R_{ct}}{R_{ct} - jX} \tag{1}$$

where $X = \frac{1}{2\pi f C_{dl}}$: reactance of the double layer capacitance, *f*: frequency, C_{dl}: double layer capacitance, and R_{ct}: charge transfer resistance. R_{ct} is evaluated as the inverse of the derivative of the current density through it respect overpotential falling upon it. The relationship between the current density and the overpotential is known as the Butler–Volmer equation. Z_p is a function of the applied overpotential because R_{ct} depends on the applied overpotential.

The components of the circuit in Fig. 3 have discrete values which depend on the "*n*" step number.

In order to obtain a continuous circuit, we assume that each level is a stage of a distributed parameter model, just like a long transmission line, and the discrete variable "*n*" is replaced by the continuous variable "*x*".

The x relative variable indicates the distance from the double layer charge, without including it, to infinity which in practice corresponds to a point within the solution but away from the electrode. The characteristics of the new continuous model shown in Fig. 4 are:where $R_e(x) = \frac{a^x R}{N^x}$: series electrolytic resistance, $Z_{pi}(x) = \frac{Z_p}{N^x}$: parallel impedance at each fractal level, Z_0: net impedance at $x=0$, $Z(x)$: partial right impedance for each fractal level,

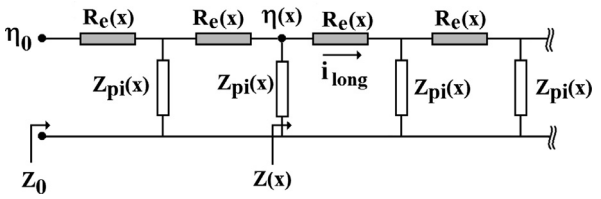

Fig. 4. Generalized continuous model of Fig. 3. Z_0: total impedance, $Z(x)$: partial right impedance for each fractal level, η_0: overpotential applied to the fractal net, and $\eta(x)$: overpotential in each fractal level.

η_0 and $\eta(x)$: overpotential applied to the net and at each fractal level respectively.

In the circuit of Fig. 4, the relationship between the overpotential $\eta(x)$ and the impedance $Z(x)$ at each level is:

$$\eta(\mathrm{x}) = \eta_0 \frac{Z(\mathrm{x})}{Z_0} \tag{2}$$

In order to obtain $\eta(x)$, a differential equation of circuit of Fig. 4 will be deduced. Consider i_{long} current as the longitudinal variation of the voltage divided in the longitudinal resistance,

$$i_{long} = \frac{1}{a^{\mathrm{x}}\mathrm{R}/\mathrm{N}^{\mathrm{x}}} \frac{d\eta(\mathrm{x})}{d\mathrm{x}} \tag{3}$$

The current which circulates in every stage through $Z_{\mathrm{pi}}(x)$ can also be interpreted as an i_{long} longitudinal variation, as follows:

$$\frac{di_{long}}{d\mathrm{x}} = \frac{\eta(x)}{Z_p/N^{\mathrm{X}}} \tag{4}$$

Z_{p} includes C_{dl}, and its value depends on the model assumed for C_{dl}. C_{dl} is assumed constant in this paper.

A differential equation of the interface can be obtained with all the components of the interface defined. From Eqs. (3) and (4) and making $k = N/a$

$$\frac{d}{d\mathrm{x}}\left(\frac{k^{\mathrm{x}}}{R}\frac{d\eta(\mathrm{x})}{d\mathrm{x}}\right) = \frac{\eta(\mathrm{x})N^{\mathrm{x}}}{Z_p(\eta(\mathrm{x}))} \tag{5}$$

Deriving the term between parentheses and simplifying, it find the final expression for the differential equation:

$$\frac{d^2\eta(\mathrm{x})}{d\mathrm{x}^2} + \ln(k)\frac{d\eta(\mathrm{x})}{d\mathrm{x}} = \frac{\eta(\mathrm{x})a^{\mathrm{x}}R}{Z_p(\eta(\mathrm{x}))} \tag{6}$$

where $\ln(k)$ gives the natural logarithm of k.

3. Model evaluation

Eq. (6) is a non homogeneous second order differential equation with constant coefficients. In order to evaluate the model and due to the complexity of the equation, it will be analyzed in a simplified version.

Overpotentials lower than 10 mV are assumed, where R_{ct} and C_{dl} are constant at any level and they do not depend on the applied voltage. Differential equation (7) is obtained from these simplifications.

$$\frac{d^2\eta(\mathrm{x})}{d\mathrm{x}^2} + \ln(k)\frac{d\eta(\mathrm{x})}{d\mathrm{x}} = \frac{R}{Z_p}a^{\mathrm{x}}\eta(x) \tag{7}$$

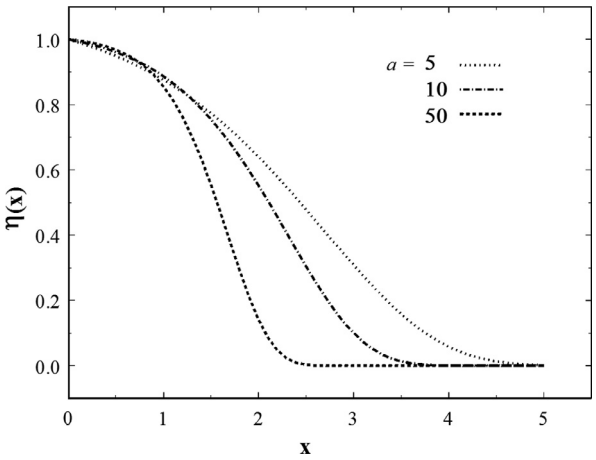

Fig. 5. $|\eta(x)|$ as a function of x obtained for different "a" values, where $R = 100\,\Omega$, $R_{\mathrm{ct}} = 10{,}000\,\Omega$, $N = 2$, $C_{\mathrm{dl}} = 3.10^{-6}$ F, $f = 0$, and $V_0 = 1$ V.

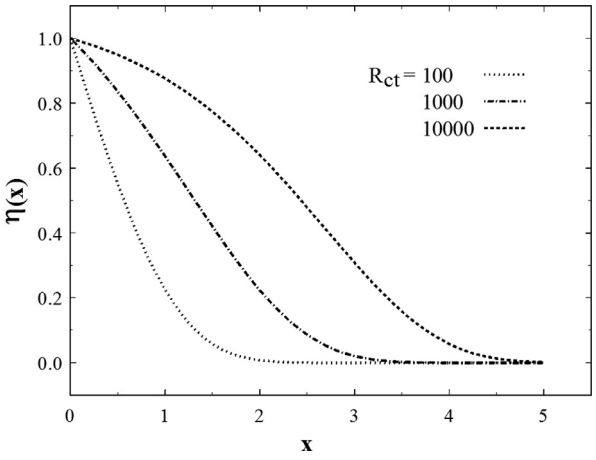

Fig. 6. $|\eta(x)|$ as a function of x obtained for different "R_{ct}" values, where $R = 100\,\Omega$, $N = 2$, $a = 5$, $C_{\mathrm{dl}} = 3.10^{-6}$ F, $f = 0$, and $V_0 = 1$ V.

Eq. (8) is the solution to the differential equation (7). Eq. (8) is based on the modified Bessel function of the second kind with the boundary condition given by $\eta(0) = V_0$.

$$\eta(\mathrm{x}) = \frac{\mathrm{v_o}k^{\frac{\mathrm{x}}{2}}\,BesselK\left(\frac{\ln[k]}{\ln[a]}, \frac{2\sqrt{a^{\mathrm{x}}R}}{\ln[a]\sqrt{Z_p}}\right)}{BesselK\left(\frac{\ln[k]}{\ln[a]}, \frac{2\sqrt{R}}{\ln[a]\sqrt{Z_p}}\right)} \tag{8}$$

Fig. 5 shows the magnitude of $\eta(x)$ for different values of a parameter, where $R = 100\,\Omega$, $R_{\mathrm{ct}} = 10{,}000\,\Omega$, $N = 2$, $C_{\mathrm{dl}} = 3.10^{-6}$ F, $f = 0$, and $\mathrm{V_0} = 1$ V. Fig. 6 shows the magnitude of $\eta(x)$ for different values of "R_{ct}" parameter, using $R = 100\,\Omega$, $N = 2$, $a = 5$, $C_{\mathrm{dl}} = 3.10^{-6}$ F, $f = 0$, and $V_0 = 1$ V. Fig. 7 shows the magnitude of $\eta(x)$ for different values of "$\mathrm{V_0}$" parameter, using $R = 100\,\Omega$, $R_{\mathrm{ct}} = 10{,}000\,\Omega$, $N = 2$, $a = 5$, $C_{\mathrm{dl}} = 3.10^{-6}$ F, and $f = 0$.Fig. 8 shows the magnitude of $\eta(x)$ for different values of "f" parameter, using $R = 100\,\Omega$, $N = 2$, $a = 5$, $C_{\mathrm{dl}} = 3.10^{-6}$ F, and $R_{\mathrm{ct}} = 10{,}000\,\Omega$.

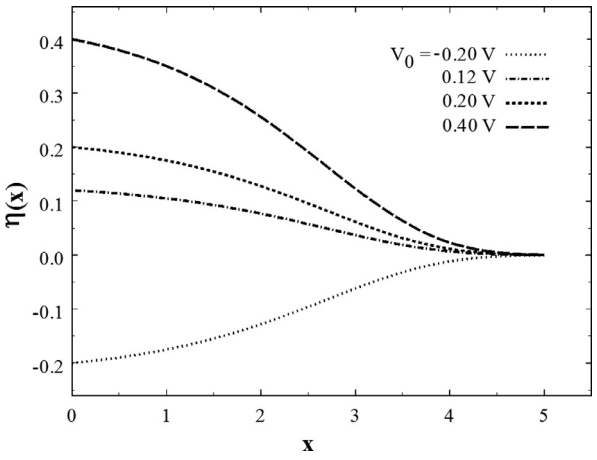

Fig. 7. $|\eta(x)|$ as a function of x obtained for different "V_0" values, where $R = 100\,\Omega$, $R_{ct} = 10{,}000\,\Omega$, $N = 2$, $a = 5$, $C_{dl} = 3.10^{-6}$ F, and $f = 0$.

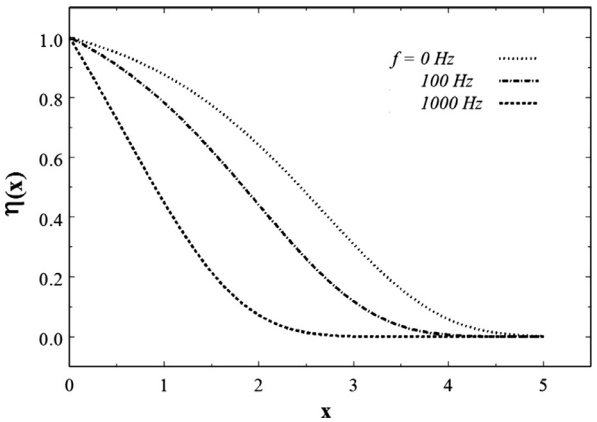

Fig. 8. $|\eta(x)|$ as a function of x obtained for different "f" values, where $R = 100\,\Omega$, $N = 2$, $a = 5$, $C_{dl} = 3.10^{-6}$ F, and $R_{ct} = 10{,}000\,\Omega$.

Fig. 9 shows the phase angle of $\eta(x)$ for two different "f" values, using $R = 100\,\Omega$, $N = 2$, $a = 5$, $C_{dl} = 3.10^{-6}$ F, and $R_{ct} = 10{,}000\,\Omega$.

4. Discussion

In this paper, an electrode–electrolyte interface has been modeled with a continuous fractal structure based on quadrupoles. A transformation of an "n" step number discrete variable in a continuous variable x has been proposed.

In order to know how to interpret the physical meaning of a fractal, when a continuous variable is used, the same reasoning as in long transmission line has been applied. It must consider the fractal as a continuous series of quadrupoles, where each is a combination of electrolytic resistance and parallel impedance of each level.

In Fig. 5 it can be seen that the parametric curves have more slope as "a" grows. This effect is due to an increase in electrolytic resistance of the branches. Likewise, the raising slopes of parametric curves of Fig. 6, when R_{ct} decrease, are due to the decrease of Z_{pi} impedance. Both effects increase the rate of fall of potential along the transmission line.

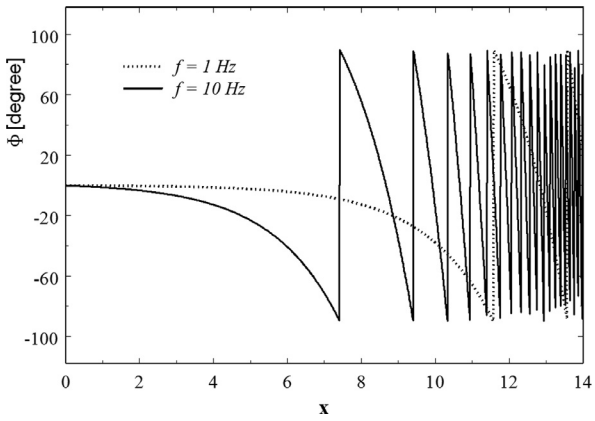

Fig. 9. Phase angle of $\eta(x)$ as a function of x obtained for two different "f" values, using $R = 100\,\Omega$, $N = 2$, $a = 5$, $C_{dl} = 3.10^{-6}$ F, and $R_{ct} = 10{,}000\,\Omega$.

The rapid decreasing of potential in Figs. 5 and 6, after a small number of stages ($x < 6$), is very important, because in any real system there can only be a finite number of fractal levels. This observation is similar to that reported by other authors [8,9]. In Fig. 7 the different curves correspond to the different overpotentials applied, as marked in the figure. At a sufficiently long distance from the surface, the potential tends to 0 independently of the overpotential applied.

The proposed continuous model predicts the potential variation with the distance to electrode due to the material's roughness—i.e.: geometrical and morphological of surface's structure—; but it cannot predict the potential variation inside the double layer itself. Furthermore, in this work we do not calculate total interface impedance. Only potential drop at interface roughness is considered, unlike Dr. McAdams et al.'s review [14] where total electrode–electrolyte impedance is modeled through Randles, McAdams, Constant Phase Angle, Levie, Liu, Nyikos and Pajkossy models among others.

Nevertheless, we might say that the use of an analytical solution of differential equation, as a fractal continuum model, instead of infinite continued fractions, represents an improvement against Dr. McAdams impedance models review. But we emphasize, that we do not model impedance, only Ohmic potential drops in the roughness of the electrode.

A comparison between our simulations and experimental results would be the curves presented in the work of Woo et al. [10] and Yoon et al. [11]. In these works, the curves are qualitatively similar to ours, but show different phenomena. According to the authors, despite working with large external overpotential applied—among 0 and 400 mV—involving Ohmic potential drops in the roughness of the electrode, these are not important because the roughness is at least ten times less than the thickness of the double layer.

Therefore in these works, the potential curves versus distance reflect the potential drop on the double layer.

Woo used as working electrode "a flame-annealed Au (111) film deposited on glass" whose roughness is on the

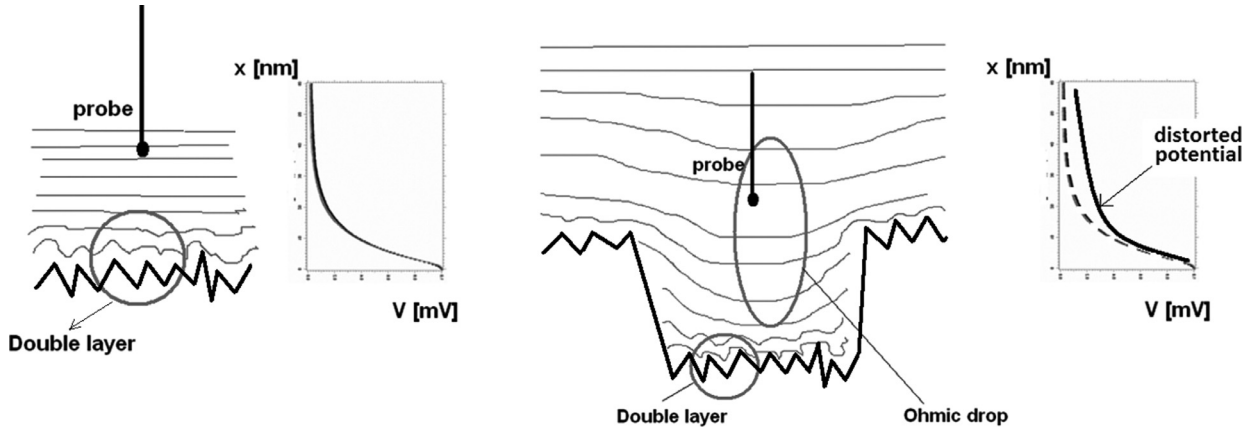

Fig. 10. Left: Schematic of flat surface with Rq = 1 nm, and his potential vs. distance curve. Right: Schematic of rough surface with Rq >> 1 nm, and his distorted potential vs. distance curve.

order of nm. Electrolytic solutions containing different concentrations of $NaBF_4$ were used. The reason of this election is that these solutions show no appreciable specific adsorption on gold surfaces.

This means that Coulomb forces prevail over the short range forces. While Yoon also used an "Au (111) film deposited on glass" as working electrode, his electrolytic solutions contained different concentrations of $NaClO_4$. As in Woo's experiments, the choice of electrolytic solutions is based on the fact that the ions Na^+ and ClO_4^- have negligible specific adsorption on gold surfaces.

In both cases the experiment consisted of slowly advancing a probe—electrochemically etched gold wire, coated with an insulator material except its apex—to the working electrode until making contact with the surface of WE.

Also in both cases, it could be considered that the equivalent electric model is a R–C_{dl} series, since it is assumed that there is no specific adsorption of electrolytes, or electrochemically active species participating in charge transfer.

Measurements show that potential drops, depend heavily on the concentration of the electrolyte solution. For concentrations of 1 mM of both $NaClO_4$ and $NaBF_4$, no-effects on the double layer were observed, for distances greater than 20 nm.

Curves qualitatively similar to the present work are shown by Hurth et al. [12]. It is possible that these curves representing the combined effects of roughness and double layer, because the size of the double layer is of the same order of roughness.

Hurth's experiments consisted of slowly advancing a nanometric probe made of PtIr wire ($\phi \approx 400$ nm) to a Pt foil of 0.2 cm^2 ($\approx 4.5 \times 4.5$ mm). As electrolyte, he used KCl. The variations shown of $V(x)$ as a function of electrode distance extend to 60 nm. Hurt´s experiment showed an abnormality: $V(x)$ did not show changes when different external overpotentials were applied in a solution of 10 μM KCl, with a double layer thickness greater than 60 nm.

Regarding to roughness effect on measurements, first we have to highlight that Hurth's Pt foil has a local root mean square average of the roughness profile ordinates Rq = 1.35 nm. Although Hurth's study does not mention it, we can assume that this value is valid for surfaces of around 10 μm^2 if we consider Blackstock et al. work [15], where a 1 Å roughness is valid for 1 μm^2 surface. The area of Hurth's Pt foil is 20 mm^2, which is 1,000,000 times bigger than the assumed area. To understand why surrounding surfaces could disturb local potential measurements, first we have to analyze Hurth's assay.

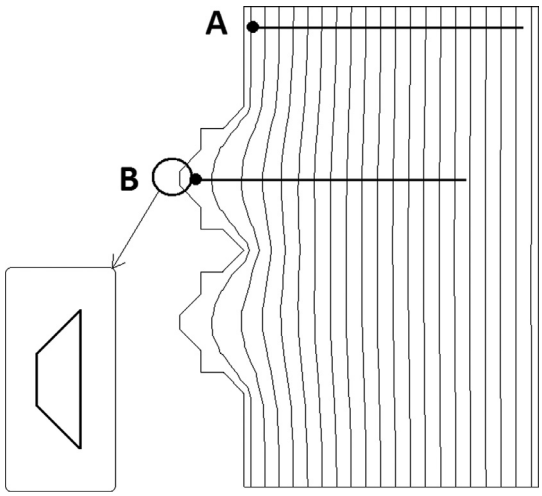

Fig. 11. Equipotential lines in a fractal electrode by using Quick Field simulation. Each line = 0.05 V; left electrode = 1 V, right electrode = 0 V.

When a test probe gets closer to this surface, it moves through equipotential surfaces, to which surrounding structures also contribute. Following Fig. 10 shows a side view schematic, where equipotential surfaces are visualized as equipotential lines. Figure on the left shows a 1 μm^2 surface with Rq = 1 nm but assuming that whole Pt foil has the same Rq value. Figure on the right shows a local 1 μm^2 surface with Rq = 1 nm, but as in this case surrounding bigger structures are considered, Rq could be 10–100 times greater.

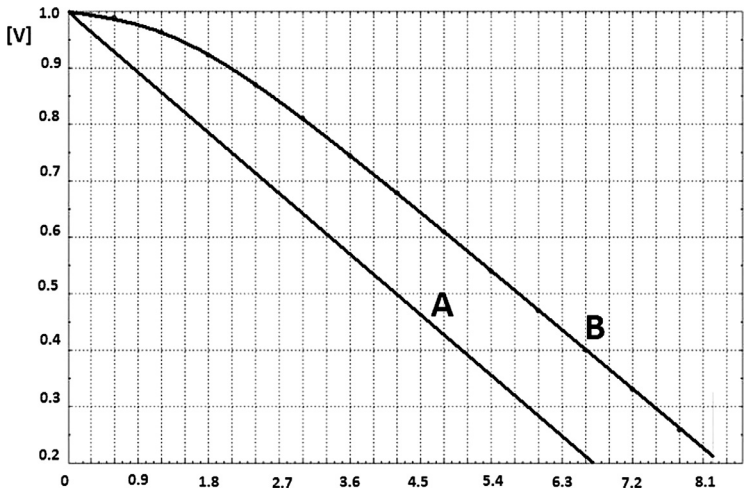

Fig. 12. Potential vs. distance curves at points A and B of Fig. 11.

When net charge transference exists at electrodes interface, Ohmic drop is overlapped with the potential measured by the PtIr probe at the double layer, so that a distortion of this value is produced.

In order to increase the support of our arguments, we evaluated through Quick Field a simulation of the proposed schematic at Fig. 11, considering only Ohmic drops. Following Fig. 11 shows a rough electrode at 1 V, with a 0 V reference on the right side. The medium is saline solution with relative permittivity $\varepsilon = 77$. A double layer is not considered.

Red circles indicate regions where the probe performs measurements. At point A, the measured potential is not affected by roughness whereas at point B the measured potential depends on surrounding roughness although the contact point probe-electrode is plain. At Fig. 12 it is observed the potential drops at points A and B.

Furthermore, it must be highlighted the similarities between our Fig. 7 and Woo's Fig. 2, but in our case with potential drops only due to Ohmic drops. This also supports the idea of potential measurements reflecting Ohmic drops, instead of a double layer. The same situation could happen in Woo's experiment [10], if the potential curves are normalized for different bias voltages. Woo´s normalized potential curves show no dependence on bias voltage, for voltage values ranging from −200 to +400 mV. It could be explained, if measurements reflect only Ohmic drops inside the fractal, like in our circuit of Fig. 4. This circuit turns on purely resistive, when large overpotentials (−200 to +400 mV) are applied, so that $R_{ct} << X$ and consequently the double layer reactance is short-circuited. Because this circuit is purely resistive, the normalized potential curves are similar to each other, and reflect only Ohmic drops.

5. Conclusion

We have presented a new theoretical tool to analyze the potential drop inside a rough electrode–electrolyte interface. Our main contribution is to use a new model based in a continuous fractal. This model is represented by a non-homogeneous second order differential equation with constant coefficients. The continuous fractal is proposed as an improvement of discrete level fractal models. The theory developed here, could be employed in the design of biosensors, fuel cells, microelectrodes, solar cells, batteries and other possible applications.

Acknowledgments

Grants given by the Agencia Nacional de Promoción Científica y Tecnológica (ANPCyT; PICT 2009-0087), el Consejo Nacional de Investigaciones Científicas y Técnicas (CONICET; PIP 112-201101-01154), el Consejo de Investigaciones de la Universidad Nacional de Tucumán (CIUNT, 26E522) with institutional funds INSIBIO (Instituto Superior de Investigaciones Biológicas). The authors would like to thank Professor Micaela García for her help in the language editing of this manuscript.

References

[1] Felice CJ, Valentinuzzi ME. Medium and interface components in impedance microbiology. IEEE Trans. Biomed. Eng. 1999;46(12):1483–7.
[2] Treo EF, Felice CJ. Non-linear dielectric spectroscopy of microbiological suspensions. Biomed Eng Online 2009;8:19.
[3] Felice CJ, Madrid RE, Valentinuzzi ME. Signal pick-up. Chapter 4 in understanding the human machine. A primer for bioengineering. Series on biomaterials and bioengineering, Vol. 4. Editado por World Scientific Publishers Co. Pte. Ltd.; 2004. ISBN 981-238-930-X p. 271–98.
[4] Ruiz GA, Felice CJ, Valentinuzzi ME. Non-linear response of electrode–electrolyte interface at high current density. Chaos Solitons Fractals 2005;25:649–54.
[5] Ruiz G, Felice CJ. Non-linear response of an electrode–electrolyte interface impedance with the frequency. Chaos Solitons Fractals 2007;31(2):327–35 (January).
[6] Wait JV, Huelsman LP, Granino AK, Korn GA. Introduction to operational amplifier theory and applications (McGraw-Hill series in electrical engineering). Mcgraw-Hill College; 1991. 2 Sub edition (October 1 p. 480.
[7] Nyikos L, Pajkossy T. Fractal dimension and fractional power frequency-dependent impedance of blocking electrodes. Electrochem Acta 1985;30(11):1533–40.
[8] Kaplan T. Effect of disorder on a fractal model for the ac response of a rough interface. Phys Rev B Condens Matter 1985;32(11):7360–6.

[9] Ramus-Serment C, Moreau X, Nouillant M, Oustaloup A, Levron F. Generalised approach on fractional response of fractal networks. Chaos Solitons Fractals 2002;14:479–88.
[10] Woo D-H, Yoo J-S, Park S-M, Jeon IC, Kang H. Direct Probing into the electrochemical interface using a novel potential probe: Au(111) electrode/$NaBF_4$ solution interface. Bull. Korean Chem. Soc. 2004;25(4):577–80.
[11] Yoon Y-H, Woo D-H, Shin T, Chung TD, Kang H. Real-space investigation of electrical double layers. Potential gradient measurement with a nanometer potential probe. J. Phys. Chem. C 2011;115:17384–91.
[12] Hurth C, Li C, Bard AJ. Direct probing of electrical double layers by scanning electrochemical potential microscopy. J. Phys. Chem. C 2007;111:4620–7.
[13] Liu SH. Fractal model for the ac response of a rough interface. Phys. Rev. Lett. 1985;55(5):529–32.
[14] McAdams ET, Lackermeier A, McLaughlin JA, Macken D, Jossinet J. The linear and non-linear electrical properties of the electrode–electrolyte interface. Biosens. Bioelectron. 1995;10(1):67–74.
[15] Blackstock JJ, Li Z, Freeman MR, Stewart DR. Ultra-flat platinum surfaces from template-stripping of sputter deposited films. Surf. Sci. 2003;546(2):87–96.